DOI 10.1007/s11182-015-0574-x

Russian Physics Journal, Vol. 58, No. 6, October, 2015 (Russian Original No. 6, June, 2015)

INVESTIGATION OF TORSIONAL STRENGTH OF THE VT6 WELD JOINT PRODUCED BY LINEAR FRICTION WELDING

G. R. Suleimanova,[1] R. R. Kabirov,[2] M. V. Karavaeva,[1] Yu. A. Ershova,[3] and A. P. Zhilyaev[2]

UDC 669.295:621.791.14

Results of measurement of torsional strength of the weld joint of the VT6 titanium alloy produced by linear friction welding are presented. For a comparison, the same method was used to test monolithic specimens of the VT6 alloy. Torsional strength values of the weld joint (τ_{US} = 861 MPa and φ = 110°) correspond to the strength of the monolithic material. In this case, the specimens fail along the base metal.

Keywords: linear friction welding, titanium alloy, torsion test.

INTRODUCTION

Linear friction welding (LFW) is a method of joining parts of machines and billets in the solid state in which heat liberated as a result of friction is used to produce a weld joint. The process of forming a one-piece joint using LFW can conditionally be subdivided into several stages [1, 2]. In the initial stage, the surfaces being joined come into contact under the action of axial loading (Fig. 1). Then under the influence of friction forces between billets, heat is liberated in the contact zone causing plasticization of thin layers of the material adjacent to the joint line. In the third stage, the plasticized layers are extruded from the joint under the effect of axial loading and form the so-called *burr*. Together with the burr, various nonmetallic inclusions and pollutants of the metal surface, forming juvenile surfaces, are extruded; as a result, in the fourth stage interatomic bonds are formed together with a one-piece weld joint under the application of an axial force in the absence of friction.

Joining titanium alloys by conventional methods of fusion welding calls for the application of some protective gases to reduce weld joint pollution in the process of liquid phase treatment. In addition, the joints of titanium alloys obtained by the method of arc welding lose their plasticity in comparison with the initial material due to the formation of a martensitic structure and its subsequent coarsening in the region adjacent to the joint [3–5]. Linear friction welding widely used to join dissimilar materials, including steel, aluminum, titanium, and intermetallic alloys, is free from these disadvantages. It can be used to join gear wheels, chains, hinges, wheels of turbines, electric buses, and bimetallic cutter blades as well as to replace damaged compressor blades [6].

In the last few years, increasing importance has been attributed to a study of weld joint fracture and influence of various structural and technological factors on the fracture characteristics [7]. Investigation of the strength of weld joints is an important and urgent problem. The weld joints are traditionally tested on tension, compression, and-or bending; however, the characteristics obtained during such tests incompletely reflect the stressed state arising during system operation. Additional data can be provided by investigations of the torsional strength of materials. However, the works devoted to investigation of the mechanical properties of weld joints by the torsion method are few in number in the literature.

[1]Ufa State Aviation Technical University, Ufa, Russia, e-mail: guzel.suleymanova@bk.ru; karma11@mail.ru; [2]Institute of Metals Superplasticity Problems of the Russian Academy of Sciences, Ufa, Russia, e-mail: kabirovr@imsp.ru; AlexZ@anrb.ru; [3]JSC "Ufa Engine Industrial Association," Ufa, Russia, e-mail: yu_ershova@mail.ru. Translated from Izvestiya Vysshikh Uchebnykh Zavedenii, Fizika, No. 6, pp. 67–73, June, 2015. Original article submitted March 6, 2015.

TABLE 1. Main Technological Regimes of Welding

Main Technological Parameters						
Vibration frequency, Hz	Amplitude of vibrations, mm	Friction force, kN	Forging force, kN	Shrinkage, mm	Welding time, s	Pressure, MPa
50	2	35	35	4	~1.5	100

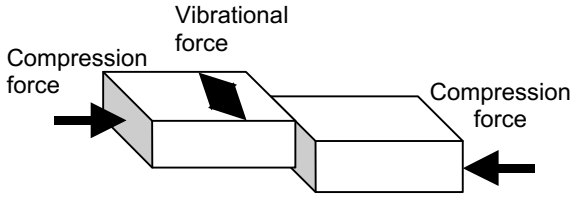

Fig. 1. Scheme of LFW.

The purpose of the present work is the determination of the torsional strength characteristics of the VT6/VT6 weld joint. Since the failure most clearly reflects the structure and properties of the material in the local volume in which the fracture proceeds, fractograms of fractured surfaces are also investigated.

MATERIALS AND METHOD OF RESEARCH

We investigated titanium VT6 belonging to high-strength two-phase martensitic titanium alloys. The base alloying elements in this alloy are aluminum (6%) and vanadium (4.5%) [8]. To investigate the weldability of VT6 with VT6, parallelepiped specimens 35 mm high having cross section 13×26 mm^2 were used. Mechanically treated billets were made from hot rolled bar according to IS 1 90006-86. Before welding, the VT6 alloys were subjected to rolling with reduction of 45–50% and subsequent annealing at a temperature of (800 ± 10)°C.

Among the main preset parameters determining the welding process were the frequency, amplitude of vibrations, rolling and shrinkage forces, time of welding, and amount of shrinkage. The parameters of the LFW process of the specimens used in the present work are presented in Table 1.

Tests for torsion were performed according to GOST 3565-80 [9]. For this purpose, specimens with a cylindrical working part having the diameter $d = 3$ mm and the calculated length $L = 15$ mm with heads at the ends for fastening in grips of a test machine Instron were manufactured. The mechanical characteristics were calculated in accordance with GOST 3565-80. To elucidate the structure, the prepared microsections etched with a solution of fluoric and nitric acids in water were used. The microstructure was investigated using an Olympus GX-51 optical microscope and a TescanMira 3 LMH scanning electron microscope. The microhardness was measured using a Duramin-1/-2 microhardness tester with a step of 0.5 mm and a load of 2 N applied for 10 s. The x-ray structure analysis was performed with a DRON-3M diffractometer using CuK_α radiation. All measurements were carried out for a welded VT6/VT6 specimen in four zones, including the joint zone, the zone of thermomechanical effect (ZTME), the zone of thermal effect (ZTE), and the base metal zone.

RESULTS OF INVESTIGATIONS

Microstructure

Figure 2 shows photomicrographs of structures in transverse cross sections of the weld joint. Investigation of the welded structure demonstrated the presence of four zones: 1) recrystallized (joint zone), 2) ZTME, 3) ZTE, and

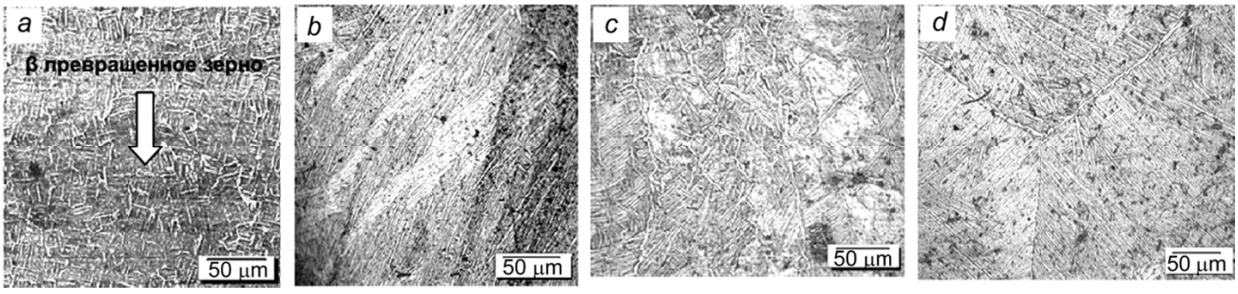

Fig. 2. Microstructure of zones including joint (*a*), ZTME (*b*), ZTE (*c*), and base metal (*d*).

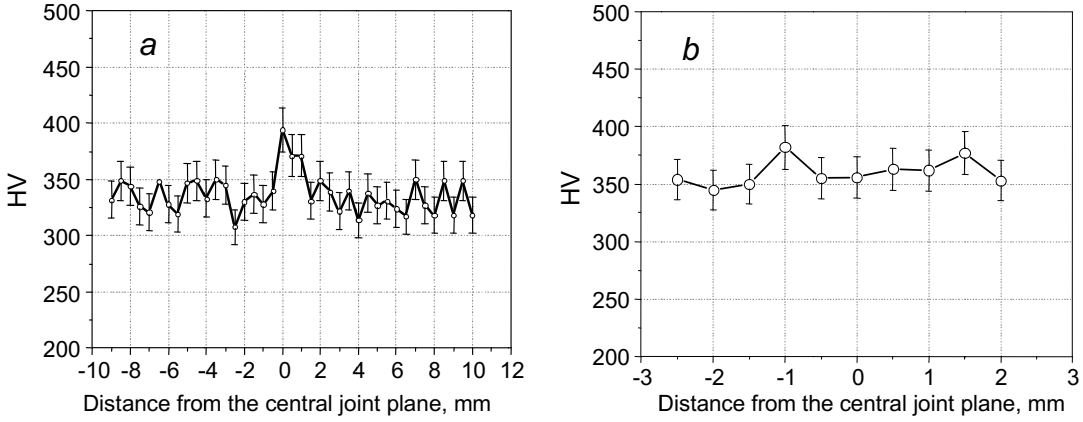

Fig. 3. Microhardness distribution for the weld joint *(a*) and initial VT6 material (*b*).

4) base metal. In the joint zone (Fig. 2*a*) in which the heating temperature corresponded to the single-phase β-region, large and practically equiaxial recrystallized grains of the β-transformed phase formed during fast cooling after the termination of the plastic deformation of metal under the action of the vibrational force (back and forth motions) during welding in the process of increasing the heating temperature as a result of action of the friction forces were observed. They have the structure of *basket weaving* formed in the process of deformation near the As3 (882°C) temperature [8]. The prevailing size of the phase components was 12 μm. Within the limits of the recrystallized β-grains, the fine needle martensitic structure was observed. In the ZTME (Fig. 2*b*), α-phase grains can be seen elongated in the deformation direction; no boundaries of the initial β-phase are observed. The region is characterized by the metallographic structure, namely, the metal grains are elongated in the direction perpendicular to the axis of load application, that is, along the direction of vibrational force. Such structure is a consequence of noticeable plastic deformation in the two-phase (α + β) region.

Here ZTE (Fig. 2*c*) is the zone where the transition from the base metal without deformation to the zone of strong plastic deformation occurs. Here a small rotation of the metal fibers in the direction of action of the friction force was observed during welding. In the microstructure of the base metal zone (Fig. 2*d*), thin-plate precipitations of the α-phase are distinguished. In this zone, the material does not experience thermal and mechanical actions; therefore, the structure does not change noticeably and corresponds to the initial state (rolling with subsequent annealing at 800°C).

Microhardness

Figure 3 shows the measured microhardness of the VT6/VT6 joint with shrinkage of 4 mm and the base metal. Microhardness in the joint zone (Fig. 3*a*) was maximum, which was explained by the formation of the fine-needle

TABLE 2. Lattice Parameters (a and c), CSD Size (d), and Microstresses ($<\varepsilon^2>^{1/2}$) in the Indicated Zones of the VT6/VT6 Weld Joint

Zone	a, Å	$\pm\Delta a$, Å	c, Å	Δc, Å	d, nm	$\pm\Delta d$, nm	$<\varepsilon^2>^{1/2}\cdot 10^3$	$\pm\Delta<\varepsilon^2>^{1/2}\cdot 10^3$
Joint	2.928144	0.000025	4.667944	0.000103	81.0	3.8	2.16	0.09
ZTE	2.926674	0.000027	4.671081	0.000073	78.2	6.6	1.56	0.09
ZTME	2.926280	0.000022	4.671124	0.000060	79.7	2.5	1.55	0.08
Base metal	2.924408	0.000206	4.669430	0.000394	124.3	4.1	0.60	0.07

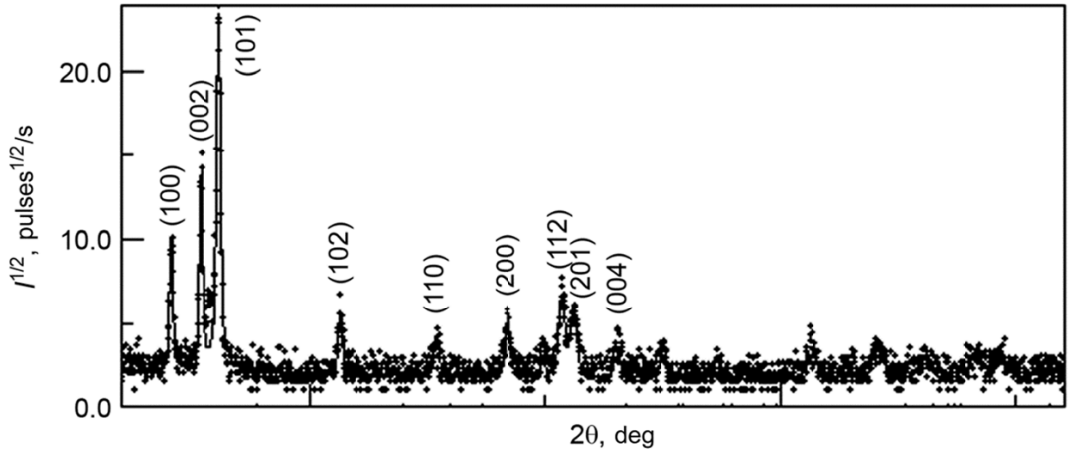

Fig. 4. X-ray diffraction pattern of the welded VT6/VT6 specimen.

martensitic structure within the limits of a small recrystallized β-grain that led to an increase in the alloy strength, which was also confirmed by the microstructural data (Fig. 2*a*). In the next zone the deformation of the materials during welding proceeded at a lower temperature in the two-phase zone, thereby leading to an increase in the defect density and hence to material hardening. The zone of the base metal did not undergo significant changes, and the microhardness was equal to that of the base VT6 material. A comparative study of the microhardness of the initial annealed specimen (Fig. 3*b*) demonstrated its sufficiently uniform distribution.

X-ray structural analysis

The x-ray diffraction pattern of a welded specimen is shown in Fig. 4. Phases with hexagonal densely packed (HDP) lattice (α'- and α-phases) prevailed. The lattice parameters (a and c), the size of the coherently scattering domains (CSDs), and the microstresses are given in Table 2.

Figure 5 shows the distribution of coherently scattering domain sizes and the dislocation density in the indicated zones. As expected, the CSD size was minimal in the joint zone, and the dislocation density was maximal in the zone directly adjacent to the joint (Fig. 5), which was also confirmed by the increased microhardness (Fig. 3*a*). The dislocation density decreased with increasing distance from the joint.

Torsion test

Figure 6 shows the fractured specimens. The fracture was observed outside of the joint and transitive zones, and the failure was observed along the base metal. Figure 7 shows the torque–twist diagrams for the torsion tests of

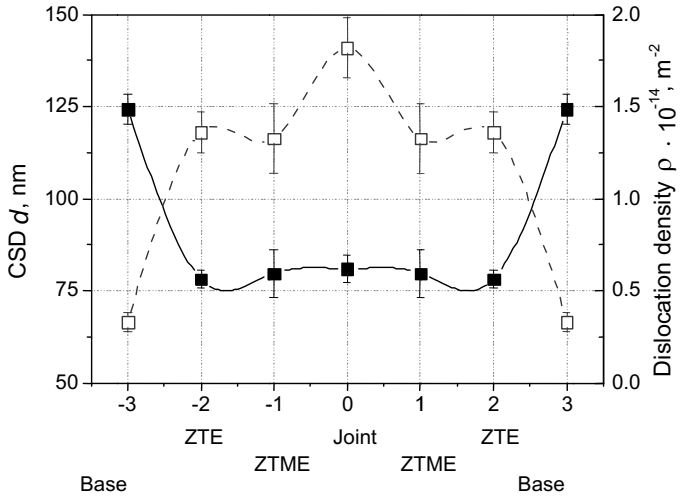

Fig. 5

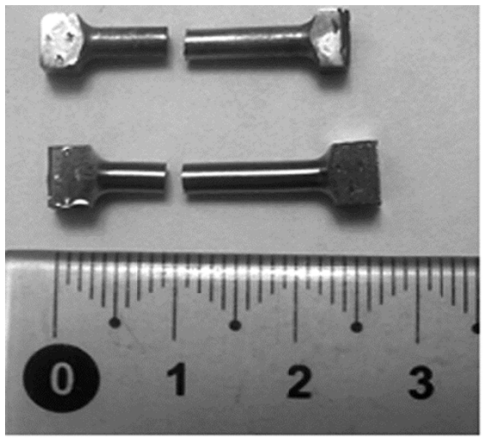

Fig. 6

Fig. 5. Changes of the CSD *d* (solid curve) and dislocation density ρ (dashed curve) in the indicated zones.

Fig. 6. Specimens after torsion test (the VT6/VT6 weld joint is shown at the top, and the monolithic specimen VT6 is shown at the bottom).

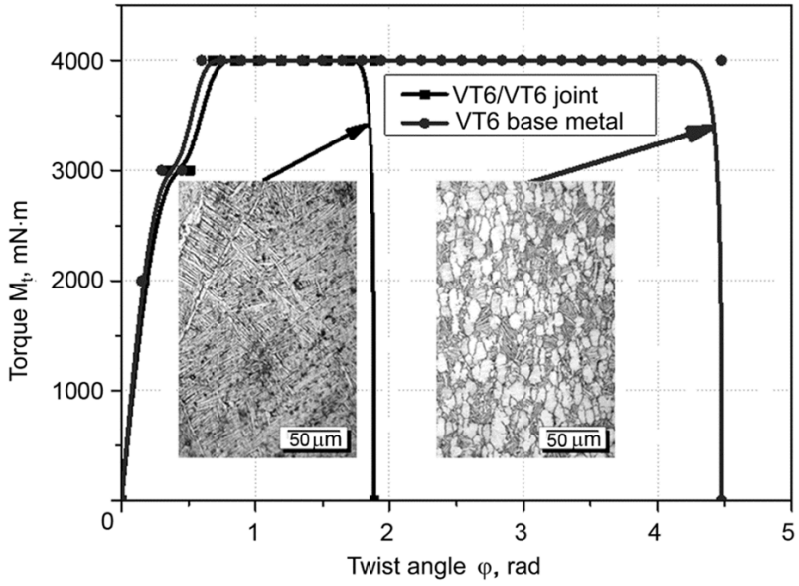

Fig. 7. Tortion-twist diagram for VT6/VT6 and VT6.

VT6/VT6 joint specimens and of the initial VT6 material. The inserts show the specimen microstructures in the zone near the failure.

As can be seen from the torsion-twist diagram, the twist angle φ before fracture of the base metal with equiaxial grain structure was larger than that of the weld joint having the plate structure. The tensile strength of the weld joint was τ_{US} = 810 MPa, and the twist angle φ before fracture was about 110° = 1.9 rad. The VT6 tensile strength was

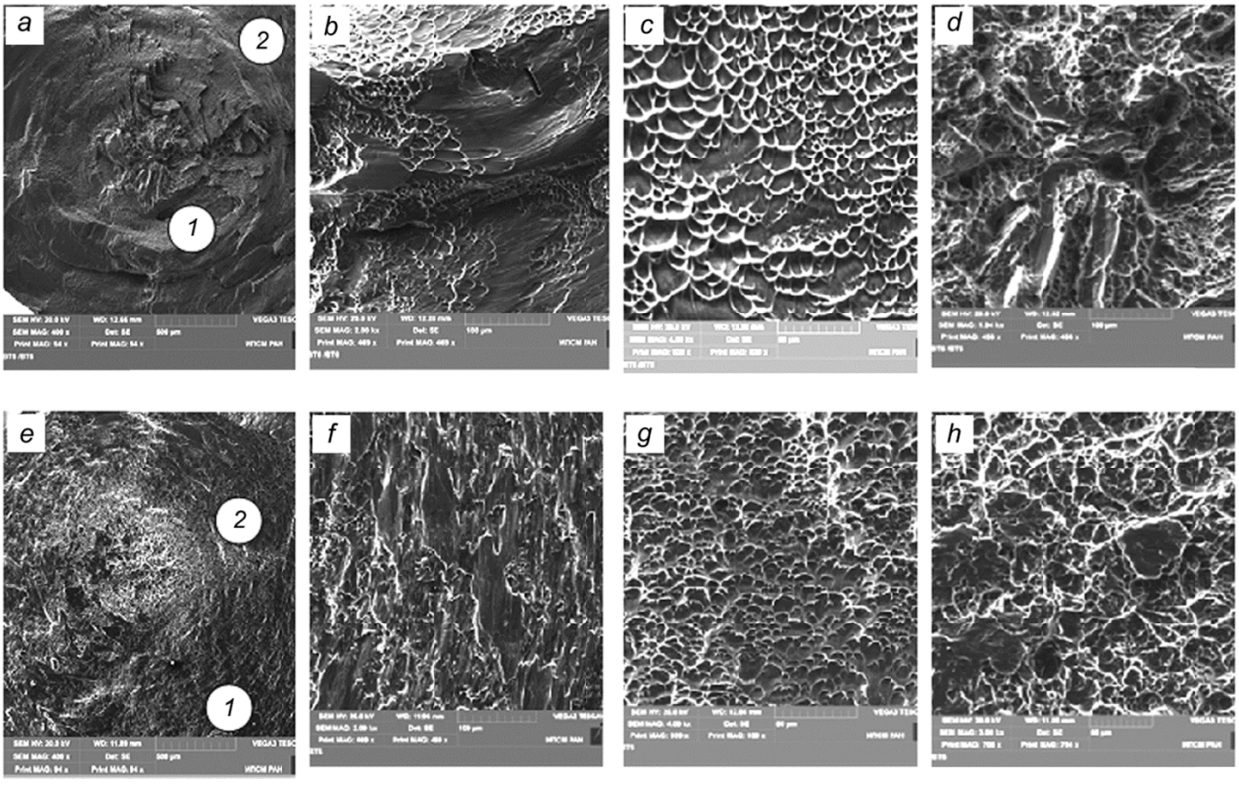

Fig. 8. Fractograms of the zones of the fracture center (*a* and *e*), viscous component (*b* and *f*), and final failure (cut) (*c* and *g*); external view of the final failure zone of the VT6/VT6 joint (*d*) and of VT6 (*h*). Here *1* indicates the final failure zone and *2* indicates the fracture center.

τ_{US} = 860 MPa, and the twist angle φ before fracture was approximately 265° = 4.5 rad. High strength properties of the joint zone are explained by the formation of the recrystallized structure comprising α'-martensite whose strength characteristics are higher than those of the base metal. The obtained strength characteristics of the weld joint under torsion allow us to conclude that the weld joint characteristics are sufficiently high and correspond to those of the monolithic material.

Fractograms

Figure 8 shows fractograms for the fractured VT6/VT6 weld joint and initial VT6 material. It can be seen that the character of fracture for both failures is viscous, but the failure surface in the monolithic material is more smoothed, which demonstrates its higher ductility in comparison with the joint. Pores are noticeable in the fractogram of the fracture center of the welded specimen (Fig. 8*a*). In the transitive viscous zone (Fig. 8*b*), the failure surface with elongated pits in the presence of such wavy relief is called *the surface smoothed under tension*, *splitting along the slip planes*, or *viscous detachment* [10]. In the final failure zone (Fig. 8*c*), pits are elongated. In the fractograms of the fracture center of the monolithic material (Fig. 8*e*), the smoothed fracture surface can be seen. In the transitive zone of the viscous component (Fig. 8*f*), traces of ripples or of the so-called serpentine slip characterize the microlocal character of plastic deformation and demonstrate high ductility of fracture.

During torsion, equiaxial pits were observed in the failure regions corresponding to fracture in response to normal stresses, and parabolic pits were observed in the remaining failure regions in response to tangential stresses. In the final failure zone (Fig. 8*g*), the pit relief caused by viscous plastic fracture was observed.

Investigation of the fracture histograms demonstrated that the fracture zone was characterized by viscous (fibrous) failure both for the weld joint and monolithic specimen. In the monolithic material, the bumpy smoothed relief was observed that testified to considerable plastic deformation preceeding failure. The direction of pit elongation indicated the direction of fracture development in the microvolume as well as the direction of crack front propagation. In the process of fracture pits deepen as a result of contraction of bridges between them. Small extention but sufficient depth of pits demonstrates high torsional strength of the joint and initial material.

CONCLUSIONS

In this work it has been shown that the chosen regime of linear friction welding allows a high-quality joint of the VT6 alloy to be obtained. The structural investigation of the specimens of the VT6/VT6 weld joint demonstrated the presence of the following zones in the region near the joint: recrystallization zone, strong plastic deformation (thermomechanical) zone, transitive (thermal) zone, and base metal zone. The microhardness was maximal in the joint zone, which indicated the formation of the fine-needle martensitic structure within the small recrystallized β-grain leading to the increased strength of the alloy.

The analysis of the failure surfaces demonstrated that the fracture zone was characterized by viscous (fibrous) failure, small extension, but sufficient depth of pits for both the weld joint and the monolithic specimen which demonstrated high torsional strength of the joint and initial material. The characteristics of the torsional strength ($\tau_в$ = 810 MPa and φ = 110° (1.9 rad)) confirmed sufficiently high characteristics of the weld joint corresponding to the strength of the monolithic material. In this case, fraction occurs along the base metal.

REFERENCES

1. A. Varis and M. Frost, Mat. Sci. Eng., **A271**, 477–484 (1999).
2. W.-Y. Li, T. J. Ma, S. Q. Yang, *et al*., Mater. Lett., **62**, 293–296 (2008).
3. P. E. Denney and E. A. Metzbower, Weld. J., **68**, 342s–346s (1989).
4. P. S. Liu, W. A. Baeslack, and J. Hurley, Weld. J., **73**, 175s–181s (1994).
5. W. A. Baeslack, J. Mater. Sci. Lett., **1**, 229–231 (1982).
6. P. Wanjara and M. Jahazi, Metall. Mater. Trans., **A36**, 2149–2164 (2005).
7. M. V. Karavaeva, S. K. Kiseleva, V. M. Bychkov, *et al*., Pis'ma Mater., **2**, No. 1, 40–44 (2012).
8. E. A. Borisov, Metallography of Titanium Alloys [in Russian], Metallurgiya, Moscow (1980).
9. GOST 3565-80 "Metals. Torsion Test Method."
10. T. A. Gordeeva and I. P. Zhegina, Analysis of Kinks in the Estimation of the Reliability of Materials [in Russian], Machinostroenie, Moscow (1978).